Wet Coating Deposition of ITO Coatings on Plastic Substrates

N. AL-DAHOUDI AND M.A. AEGERTER*
Institut fuer Neue Materialien—INM, Department of Coating Technology, Im Stadtwald, Gebaeude 43, 66123 Saarbruecken/Germany
aegerter@inm-gmbh.de

Abstract. In_2O_3:Sn (ITO) transparent conducting coatings of high optical quality have been obtained on glass and several plastic substrates by spin and dip coating processes followed by a low temperature processing ($T < 130^{\circ}$C). The sols are made of crystalline nanoparticles redispersable in an alcohol and modified by adding a binder to favour the coalescing of the particles and to allow the deposition of thick single layers (>400 nm). The smallest stable resistivity so far obtained is $\rho = 9 \times 10^{-2}$ Ωcm (sheet resistance of 1.6 k$\Omega_{\square}$ for a 570 nm thick single layer). The transparency in the visible range is high, $T \approx 87\%$, the abrasion resistance is in agreement with DIN 58-196-G10 and the hardness according to ASTM D 3363-92a is 1H. A spray process allows to obtain antiglare-conducting coatings with an adjustable gloss of 60 to 80 GU and an optical resolution >8 lines/mm.

Keywords: sol-gel, electrical coatings, conductivity, indium tin oxide, ITO, plastic substrate, antiglare coating, antistatic coatings, low temperature processing

1. Introduction

Transparent conducting coatings are widely used as electrodes in optoelectronic devices, as IR reflecting or heatable layer, for electromagnetic shielding or dissipating static, etc. Among the most important material are *n*-type oxide semiconductors (TCO) such as indium tin oxide (ITO) and fluorine or antimony doped tin dioxide (FTO, ATO) [1].

There is today a great interest to coat systems which do not withstand high temperature such as plastic substrates or already preformed glass devices. These above materials can only be deposited by physical deposition techniques [2]. However wet coating deposition processes such as spray, dip and spin coating are also well adapted techniques to coat even large substrates using a cheaper infrastructure if organic precursors fully polymerizable at low temperature can be incorporated in the sol formulation (organic-inorganic hybrids). For TCO coatings one possible issue is the use of hybrid sols containing a high amount of already conducting crystalline oxide nanoparticles [3].

*To whom all correspondence should be addressed.

The paper reports on recent progress to obtain ITO coatings processed at temperature as low as 130°C and their optical, electrical, mechanical and textural characteristics.

2. Experimental

2.1. Precursors and Sols

In_2O_3:Sn nanopowders with primary size adjustable up to about 20 nm and having the cubic In_2O_3 phase were prepared by a controlled growth technique. The detailed preparation can be found in [3–5]. The powders can be fully redispersed in alcohol and water. Their density is 6.45 g/cm^3 corresponding to 92% of the theoretical density of In_2O_3. They have been already used to develop nanoparticulate coatings on glass with sintering at high temperature [6, 7].

The sols used to obtain transparent conducting coatings consist of an ethanolic solution containing 25 wt% redispersed ITO nanoparticles modified by adding under ultrasonic treatment hydrolyzed 3-methacryloxypropyltrimethoxysilane (MPTS). Polymethylmetacry-

late (PMMA), polycarbonate (PC) and glass substrates were coated by spin and dip coating process. The resulting films were first cured by UV irradiation with an average intensity of 105 mW/cm^2 for 110 s (Beltron) and then heated in air or reducing atmosphere at 130°C up to 20 hours. A further annealing under forming gas or N_2 atmosphere was performed at 130°C during 3 hours to improve their electrical properties.

The same sols were used to obtain antiglare conducting coatings, but were sprayed at room temperature for a period of 15 to 20 seconds using a SATA mini-jet spray gun (0.5 mm nozzle, 3 bar) on polycarbonate or glass substrates. The coatings, a few μm thick, were then polymerized using the same process.

2.2. *Characterization of the Coatings*

2.2.1. Textural Properties. The surface morphology of the coatings was analyzed using a white light interferometer (WLI) and AFM (Zygo Newview 5000) and Scanning Electron Microscopy (SEM-JEOL 6400). Coating cross sections were observed by high resolution Transmission Electron Microscopy (HR-TEM-Philips, 200 KeV).

2.2.2. Optical Properties. Optical transmission and reflection were determined using a Variant Cary 5 E spectrophotometer in the wavelength range 300 to 3000 nm. IR spectroscopy was performed with a Bruker IFS 66V instrument. Haze, clarity and gloss were measured using a ByK Gardner plus and a micro-TRI reflectometer.

2.2.3. Mechanical Properties. The thickness (t) of the coating was determined using a Tencor P10 profilometer. The abrasion resistance and the adhesion of the coatings was tested according to DIN 58196 and their hardness according to ASTM D3363-92a.

2.2.4. Electrical Properties. The sheet resistance ($R_\square$) was measured by a 4 points technique or a contactless measurement device (Lehigton Electronic Inc.). The resistivity was calculated from $\rho = R_\square \cdot t$.

3. Results and Discussion

3.1. *Transparent Conducting Coating*

The evolution of the sheet resistance of a 570 nm thick single layer of pure ITO and MPTS/ITO (6 vol%) coatings deposited on a 3 mm thick PC substrate is shown in Fig. 1 after different annealing treatments. Whatever the treatment is, $R_\square$ for pure ITO remains high (>1 M$\Omega_\square$) and the coating adhesion is very poor. Cured MPTS/ITO coatings were found to exhibit a minimum of $R_\square$ for a composition volume ratio of 6%. After deposition, the sheet resistance is high, about 10 M$\Omega_\square$. A heat treatment in air at 130°C only slightly decreases $R_\square$ down to 7×10^5 $\Omega_\square$. IR spectroscopy shows that a well defined Si—O—Si network (1050 cm^{-1} band) is not achieved and that the presence of ITO particles impedes the polymerization and condensation processes [6]. A UV treatment drastically reduces the sheet resistance down to 8 k$\Omega_\square$. The C=C band (1036 cm^{-1}) is completely eliminated and the C=O band (1716 cm^{-1}) is strongly reduced so that a well defined Si—O—Si network link the conducting particles together leading to a much better conductivity. A further annealing in a reducing atmosphere at 130°C still lowers this value down to 800 $\Omega_\square$.

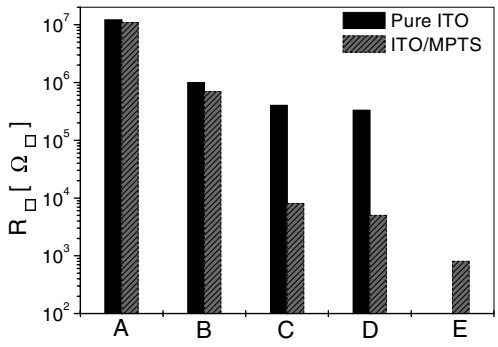

Figure 1. Sheet resistance of 570 nm thick MPTS/ITO (6 vol%) coatings measured after different heat treatments in air: 130°C, 15 h. (A) as deposited; (B) as deposited + heat treatment in air at 130°C during 10 h; (C) as deposited + UV irradiation (110 s, 105 mW/cm^3); (D) process C + heat treatment in air at 130°C/30 h; (E) process D + reducing in forming gas at 130°C/3 h.

These values, measured just after the processing of the coatings, are only stable when the coatings are kept in vacuum or in a protective atmosphere such as nitrogen or argon (Fig. 2). When kept in air the sheet resistance however slightly increases with time to reach a stable value of 1650 $\Omega_\square$ in air (20°C, 40% RH).

The mechanisms leading to these variations are not yet clear, but are certainly related to the composition and the morphology of the coatings. Besides the polymerization process of MPTS an important effect of both the UV and the reducing treatment is to diminish the concentration of chemisorbed oxygen species on the

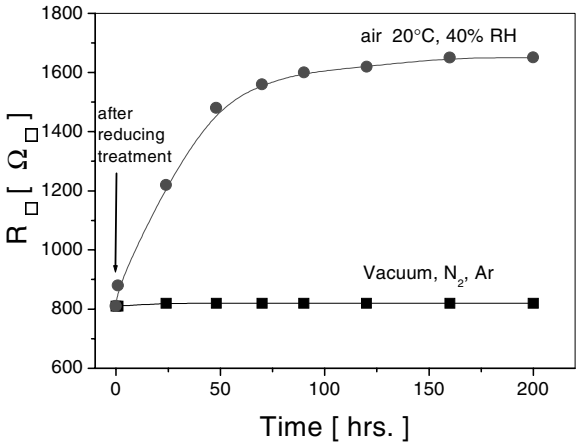

Figure 2. Time evolution of the sheet resistance of 570 nm thick MPTS (6 vol%)/ITO coatings left in a protective atmosphere (vacuum, N_2, Ar) in vacuum and air. The coatings have been initially post annealed in a reducing atmosphere.

surface of the ITO particles, which act as free electron traps surface states. This leads to an increase of the carrier concentration and consequently to a large reduction of $R_\square$. As the coatings are porous (see below), oxygen from air slowly diffuses back into the coating and is again chemisorbed at the surface grains as charged species. This leads to an electron transfer from the particles to the adsorbed species inducing a high band bending increasing the potential barrier height and consequently the resistivity. Without the presence of oxygen, the values of $R_\square$ are stable.

The surface morphology of the coatings observed by SEM (Fig. 3) consists of loosely packed globular grains (raspberry like) about 100 nm in size formed by the aggregation of the ITO nanoparticles linked together by a small strip of polymerized MPTS (dark regions). The coating roughness measured by WLI on a $53 \times 70\ \mu m^2$ area with a lateral resolution of 600 nm is $R_a = 0.85$ nm, with a peak-to-valley maximum value of $R_{PV} = 15$ nm. When measured with a higher resolution on a $1 \times 1\ \mu m^2$ area (AFM), the values are $R_a = 4$ nm and $R_{PV} = 28$ nm.

The optical transmission and reflection spectra of a 3 mm thick PC substrate uncoated and one coated with a 500 nm hybrid ITO layer is shown in Fig. 4. A high transmission of about 87% is observed in the visible range. The influence of the carrier is clearly seen by the strong absorption occurring in the near IR range (900 nm $< \lambda <$ 2000 nm) and the increase of the reflection for $\lambda > 2\mu$m.

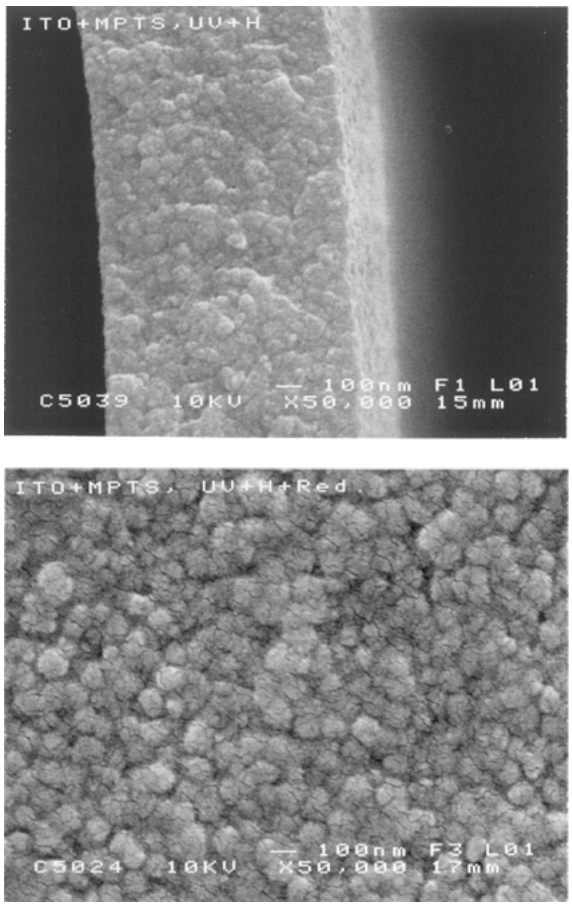

Figure 3. SEM picture of the surface (top) and HR-TEM cross-section (bottom) of a MPTS/ITO coating UV cured (110 s) and heat treated at 130°C, 15 h.

The mechanical properties of the coatings deposited on PC substrate have been studied by various test. The adhesion is in agreement with the Tape test procedure (DIN 58196-K2). No scratch (class 1) was observed after 10 rubbing cycles with an eraser under a load of 10 N (DIN 58196-G10). The hardness measured using the Pencil test ASTM D 3363-92a is 1H. Higher value were observed when the amount of MPTS was increased, but such coatings present also a higher value of the sheet resistance.

3.2. *Antiglare Conducting Coatings*

Antiglare conducting coatings have been obtained by spray coating followed by the same post deposition treatments. The spray gun delivers droplets with an

Table 1. Typical gloss, haze, clarity, resolution and abrasion resistance of antiglare coatings deposited on plastic and glass substrates and cured by UV irradiation.

Gloss @ 60°	Haze (%)	Clarity (%)	Resolution (USAF chart)	Abrasion resistance (9.8 N)
60–70	≤10	75–90	≥8 lines/mm	DIN 58196-G10

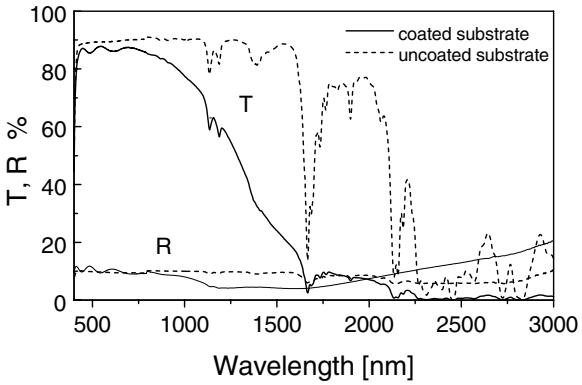

Figure 4. UV-near IR transmission (T) and reflection (R) measured against air of a 500 nm thick MPTS/ITO coating deposited on a 3 mm thick polycarbonate (PC) substrate and of an uncoated PC substrate.

Figure 5. Glaze of a white object placed in front of a AS-AG coated plastic (left) and an uncoated one (right). The picture of the building placed 2 cm behind the substrates is clearly visible in both configurations.

average size of 25 μm. When arriving on the cold substrate they spread and form a rough surface which can be polymerized following the same treatments (UV irradiation + heating at $T \approx 130^{\circ}$C). The thickness of the coatings can range up to a few μm.

The surface morphology of such coatings consist of 10 to 100 μm features confirming an average roughness of $R_a = 0.2$ μm with peak to valley of 0.8 μm. Similar sheet resistance values and mechanical properties can be obtained. Table 1 shows the results of the optical properties of the coatings.

Figure 5 shows the optical effect of such coatings. The image of the entrance of INM placed 2 cm behind a coated and a non-coated substrate is clearly visible and the glare of the object placed in front of the substrates is strongly reduced at the coated side.

4. Conclusions

Stable hybrid pastes and sols allowing the deposition of conducting, antistatic and antiglare-antistatic coatings fully processable at low temperature ($T < 130^{\circ}$C) have been developed. They have been obtained by modifying an ethanolic suspension of redispersed crystalline ITO nanoparticles with a hydrolyzed silane (MPTS) acting as a binder. Single layers as thick as 570 nm can be obtained by spin or dip coating processes on plastic (PMMA, PC) and glass substrates. The curing process involves a UV irradiation (105 mW/cm^2, 110 s) followed by a heat treatment at $T = 130^{\circ}$C during 15 h and then a reducing treatment in forming gas. 570 nm thick coatings exhibit a high transparency ($T \approx 87\%$) and a stable sheet resistance as low as 1.6 k$\Omega_{\square}$ (resistivity $\rho = 9 \times 10^{-2}$ Ωcm). The abrasion resistance is in agreement with DIN 58196-G10 class 1, the adhesion passes the tape test DIN 58196-K2 and the pencil hardness is 1 H according to ASTM D 3363-92c. The surface roughness is low, $R_a \approx 1$ nm. Antistatic coatings with similar sheet resistance presenting an antiglare effect (GU $\sim$ 65) have been obtained on the same substrates by a spray process at room temperature followed by UV irradiation and N_2 annealing. All these coatings are stable under UV or visible light irradiation and consequently their properties are presently better than those obtained with commercial conductive polymers [8]. The process can be applied to coat at low temperature ($T < 130^{\circ}$C) flat or slightly curved substrates such as CRT, LCD, PDP, touch screen panels, discharge plates in clean environment, etc.

References

1. H.L. Hartnagel, A.L. Dawar, A.K. Jain, and G. Jagdish, *Semiconducting Transparent Thin Film* (IOP Publishing, Bristol and Philadelphia, 1995).
2. H.K. Pulker, *Coatings on Glass*, 2nd edn. (Elsevier, 1999).
3. C. Goebbert, M.A. Aegerter, D. Burgard, R. Nass, and H. Schmidt,

Proc. Materials Research Society, MRS, Nanostructured Powders and their Industrial Application **520**, 293 (1998).
4. C. Goebbert. M.A. Aegerter, D. Burgard, R. Nass, and H. Schmidt, J. Mater. Chem. **9**, 253 (1999).
5. N. Al-Dahoudi, H. Bisht, C. Goebbert, T. Krajewski, and M.A. Aegerter, Thin Solid Film **392**, 299 (2001).
6. C. Goebbert, R. Nonninger, M.A. Aegerter, and H. Schmidt, *Thin Solid Film* **351**, 79 (1999).
7. C. Goebbert, H. Bisht, N. Al-Dahoudi, R. Nonninger, M.A. Aegerter, and H. Schmidt, Journal of Sol-Gel Science and Technology **19**, 201 (2000).
8. Baytron® P Technical Information.